Published in final edited form as:
Biochemistry. 2011 March 22; 50(11): 1788–1798. doi:10.1021/bi200028z.

Multiple Roles of Component Proteins in Bacterial Multicomponent Monooxygenases: Phenol Hydroxylase and Toluene/*o*-Xylene Monooxygenase from *Pseudomonas* sp. OX1[†]

Christine E. Tinberg, **Woon Ju Song**, **Viviana Izzo**, and **Stephen J. Lippard**[*]
Department of Chemistry, Massachusetts Institute of Technology, Cambridge, MA 02139

Abstract

Phenol hydroxylase (PH) and toluene/*o*-xylene monooxygenase (ToMO) from *Pseudomonas* sp. OX1 require three or four protein components to activate dioxygen for the oxidation of aromatic substrates at a carboxylate-bridged diiron center. In the present study we investigated the influence of the hydroxylases, regulatory proteins, and electron-transfer components of these systems on substrate (phenol; NADH) consumption and product (catechol; H_2O_2) generation. Single turnover experiments revealed that only complete systems containing all three or four protein components are capable of oxidizing phenol, a major substrate for both enzymes. Under ideal conditions, the hydroxylated product yield was ~50% of the diiron centers for both systems, suggesting that these enzymes operate by half-sites reactivity mechanisms. Single turnover studies indicated that the PH and ToMO electron-transfer components exert regulatory effects on substrate oxidation processes taking place at the hydroxylase actives sites, most likely through allostery. Steady state NADH consumption assays showed that the regulatory proteins facilitate the electron-transfer step in the hydrocarbon oxidation cycle in the absence of phenol. Under these conditions, electron consumption is coupled to generation of H_2O_2 in a hydroxylase-dependent manner. Mechanistic implications of these results are discussed.

Bacterial multicomponent monooxygenases (BMMs1) are remarkable enzymes that orchestrate a series of electron transfer and substrate activation events in order to prime dioxygen for donation of a single oxygen atom into a C–H bond or across a C=C double bond (1,2). Proteins belonging this family are subdivided into four classes, soluble methane monooxygenases (sMMOs), phenol hydroxylases (PHs), alkene monooxygenases (AMOs), and four-component alkene/arene monooxygenase (TMOs), based on substrate preference and sequence homology (3,4). The ability of BMMs to generate potent oxidizing species without damaging their active sites or consuming electrons in a futile manner depends on the dynamic involvement of three or more protein components: a 200-255 kDa dimeric hydroxylase that houses two copies of a carboxylate-bridged diiron catalytic center; a 38-45 kDa reductase that accepts electrons from NADH and shuttles them though its flavin and [2Fe-2S] cluster cofactors into the hydroxylase diiron sites; and a 10-16 kDa regulatory protein that couples electron consumption to hydrocarbon oxidation (1,2,5). For ToMO, an additional 12 kDa Rieske protein acts as an electron conduit between the reductase and the

[†]This work was funded by grant GM032134 from the National Institute of General Medical Sciences. CET thanks the NIH for partial support under Interdepartmental Biotechnology Training Grant T32 GM08334. VI thanks CEINGE (Biotecnologie Avanzate, Naples, Italy) for partial support.

[*]To whom correspondence should be addressed. lippard@mit.edu. Telephone: (617) 253-1892. Fax: (617) 258-8150..

SUPPORTING INFORMATION
Figures S1-S4 as described in the text (PDF). This material is available free of charge via the Internet at http://pubs.acs.org.

hydroxylase. Timely regulation of interactions between these proteins assures efficient catalysis.

The first step in catalysis by the BMM proteins is the reductive activation of O_2 at the hydroxylase diiron centers for incorporation into substrate. The most extensively studied O_2 activation pathways in BMMs are those of the soluble methane monooxygenases (sMMOs)

[1]Abbreviations:

AMO	alkene monooxygenase
BMM	bacterial multicomponent monooxygenase
C2,3O	catechol 2,3-dioxygenase
DTT	dithiothreitol
ET	electron transfer
H_{peroxo}	second peroxodiiron intermediate species of MMOH
IPTG	Isopropyl β-D-1-thiogalactopyranoside
MMOB	regulatory protein of sMMO
MMOH	hydroxylase component of sMMO
MMOR	reductase protein of sMMO
MOPS	3-(N-morpholino) propanesulfonic acid
NADH	reduced nicotinamide adenine dinucleotide
P*	first peroxodiiron intermediate species of MMOH
PAGE	polyacrylamide gel electrophoresis
PH	three component phenol hydroxylase
PHH	hydroxylase component of *Pseudomonas* sp. OX1 PH
PHM	regulatory protein component of PH
PHP	reductase component of PH
Q	di(*μ*-oxo)-diiron(IV) intermediate species of MMOH
RFQ	rapid freeze-quench
SDS	sodium dodecyl sulfate
sMMO	soluble methane monooxygenase
T2MO	toluene 2-monooxygenase system from *Burkholderia cepacia* G4
T4mo	four component toluene 4-monooxygenase system from *Pseudomonas mendocina* KR1
TMO	four-component alkene/arene monooxygenase
ToMO	four component toluene/*o*-xylene monooxygenase protein system from *Pseudomonas* sp. OX1
ToMOC	Rieske [2Fe-2S] ferredoxin component of ToMO
ToMOD	regulatory protein component of ToMO
ToMOF	reductase protein of ToMO
ToMOH	hydroxylase component of ToMO
Tris-HCl	2-amino-2-(hydroxymethyl)-1,3-propanediol hydrochloride

from *Methylococcus capsulatus* (Bath) and from *Methylosinus trichosporium* OB3B. In these systems, reaction of the diiron(II) form of the hydroxylase (MMOH) with O_2 leads to the sequential generation of two peroxodiiron(III) units, P* (6,7) and H_{peroxo} (8-10), in the presence of the regulatory protein MMOB. Subsequent transfer of one or two protons (7,11) leads to rearrangement of the iron-oxygen core and formation of Q, a di(μ-oxo)diiron(IV) species responsible for methane oxidation (8,12-14). In the absence of methane and other substrates, Q decays slowly to H_{ox} via a pathway that is not fully understood (7).

The O_2 activation pathway of toluene/*o*-xylene monooxygenase (ToMO) from *Pseudomonas* sp. OX1 was also recently investigated (15). Upon reaction of the diiron(II) form of the ToMO hydroxylase (ToMOH) with O_2 in the presence of the regulatory protein ToMOD, a diiron(III) intermediate with no obvious absorption features rapidly formed and subsequently decayed to the diiron(III) protein resting state without progressing through a stable, high-valent Q-like intermediate (15,16). The diiron(III) intermediate, with Mössbauer parameters $\delta = 0.55 \pm 0.02$ mm/s and $\Delta E_Q = 0.67 \pm 0.03$ mm/s, could be a peroxide or hydroperoxide unit (15). The spectroscopic characteristics of this species are unusual for a peroxodiiron(III) center, however, which typically exhibits $\lambda_{max} > 650$ nm, $\theta > 0.6$ mm/s, and $\Delta E_Q > 1.0$ mm/s. These notable differences suggest that the ToMO intermediate must deviate in geometry and/or protonation state from well characterized diiron(III) peroxide species, but its exact nature remains to be fully elucidated. This species is believed to be the active oxidant in the ToMO system, because rapid freeze quench (RFQ) double-mixing Mössbauer spectroscopic experiments revealed that its rate of decay is accelerated in the presence of the substrate phenol (15). Analogous investigations of the O_2 activation pathway of the hydroxylase component from *Pseudomonas* sp. OX1 phenol hydroxylase hydroxylase component (PHH) revealed a similar intermediate species in this enzyme (17).

Although the hydroxylase proteins have been definitively established to house the diiron catalytic reaction centers, the functions of the regulatory proteins of BMMs have been a source of ongoing investigation. These proteins, of which the best-studied is MMOB in sMMO, have been implicated in the O_2 activation, substrate entry, proton transfer, and electron-transfer phases of the catalytic cycles for hydrocarbon oxidation (1,2,18). The regulatory proteins increase the rates and electron coupling efficiencies of the steady-state hydroxyation reactions (19-22), modulate the redox potentials of the hydroxylase diiron site (23,24), accelerate the rates of electron transfer between the reductase and the hydroxylase (20,21), perturb the spectroscopic features of the hydroxylase active site (19,25-29), rearrange the hydroxylase iron ligands (28,30,31), promote conformational changes in the hydroxylase (21,28,30-33), gate substrate and solvent access to the hydroxylase diiron centers (30,34), alter the substrate specificity and regiospecificity of hydroxylation reactions (27,34-36), promote the binding of an active site water molecule invoked in proton transfer (30), modulate the kinetics of the reaction of reduced hydroxylase with O_2 (37), and prevent inopportune reduction of the oxygenated iron intermediates of the hydroxylase via untimely electron transfer (30-32,38). At high concentrations, the regulatory proteins inhibit steady state activity in the sMMO, PH, and toluene 4-monooxygenase (T4mo) systems (19,20,39). The ability of these small, cofactorless proteins to influence so many distinct processes clearly indicates a mechanistic complexity that is not yet fully understood. Further studies of these and other BMM regulatory components are necessary to obtain a complete picture of their functions.

Reductase protein components in the BMM systems provide electrons to the diiron centers in the hydroxylases (1,2). The sMMO reductase MMOR, however, also affects catalysis in a complicated and versatile manner, tuning the redox potentials of the hydroxylase diiron units (23,38), altering the kinetics of the reaction with O_2 (38), promoting conformational changes in the hydroxylases (32,33), and influencing how the hydroxylases interact with substrates

(27). These observations suggest that MMOR regulates catalysis in addition to providing electrons for the reductive activation of dioxygen. Whether or not this phenomenon is restricted to sMMO, or is a general feature of all BMMs, is of interest to establish and has motivated in part the present investigation.

Toluene/*o*-xylene monooxygenase and phenol hydroxylase are the first two enzymes in a pathway that allows *Pseudomonas* sp. OX1 to metabolize aromatics as its sole carbon source (Scheme 1). Enzymes involved in the upstream segment of this pathway, ToMO, PH, and catechol 2,3-dioxygenase (C2,3O), degrade aromatic molecules through oxidation reactions. Downstream '*meta*-cleavage' enzymes then cleave the modified aromatic ring and process the resulting products for entry into major metabolic pathways required for bacterial viability (39,40). Both ToMO and PH have a broad substrate specificity and oxidize a variety of aromatic hydrocarbons in addition to their native substrates, including *o*-, *m*-, and *p*-cresol, several dimethylphenols, and benzene (39,41). By comparison to the sMMO systems, little is known about how the protein components of the *Pseudomonas* sp. OX1 BMMs act together to achieve hydrocarbon oxidation. In the studies undertaken here, we explored the influences of the *Pseudomonas* sp. OX1 PH and ToMO auxiliary proteins on substrate (phenol; NADH) consumption and product (catechol; H_2O_2) formation. The results and their interpretation constitute the present report.

MATERIALS AND METHODS

General Considerations

Distilled water was deionized with a Milli-Q filtering system. Tris-HCl gradient gels (4-20%) were purchased from Bio-Rad Laboratories. Phenol and catechol were purified by vacuum-sublimation prior to use. Other reagents were purchased from Sigma Aldrich and used as received unless otherwise noted.

Protein Purification

PHH was expressed from a vector containing the *phk*, *phl*, *phn*, and *pho* genes (pGEM3Z/PHΔMΔP). Construction of this plasmid, as well as expression and purification of hydroxylase protein from this construct, will be described elsewhere (17). Plasmids containing the genes for the PH regulatory protein, PHM (pET22b(+)/PHM), and reductase, PHP (pET22b(+)/PHP), were supplied by Prof. Alberto Di Donato (Università di Napoli Federico II, Naples, Italy). PHP was expressed as described previously, except that $Fe(NH_4)_2(SO_4)_2{\cdot}6H_2O$ and IPTG were added to final concentrations of 200 μM and 75 μM, respectively, at induction (39). The resulting cell paste (~20 g) was sonicated on ice using a Branson sonifier in 30 s pulses for 12 min at 40% output in ~100 mL of 20 mM sodium phosphate pH 7.0, 1 mM DTT, and 10% glycerol (Buffer A) containing 100 U of DNaseI (New England Biolabs). Insoluble material was removed by ultracentrifugation at 183,000 x *g* for 60 min, and the supernatant was filtered through a 0.45 μm membrane and loaded onto a Q Sepharose FF column (100 mL) equilibrated in Buffer A. The column was washed with 200 mL of Buffer A, after which bound proteins were eluted in 1 L by running a linear gradient from 0.08 to 1.0 M NaCl at 1.5 mL/min. Fractions containing PHP eluted at ~350 mM NaCl and were identified by SDS-PAGE gel electrophoresis and by absorbance at 271, 340, and 459 nm. These fractions were pooled and concentrated to ~7 mL using a 30K MWCO Amicon centrifugal concentrator (Millipore). The resulting protein was loaded onto a Superdex S75 column equilibrated with Buffer A containing 0.2 M NaCl (Buffer B). Proteins were eluted by running Buffer B over the column at a flow rate of 1 mL/min. Fractions displaying an A_{271}:A_{459} ratio of 2.5 to 3 and an A_{340}:A_{459} ratio slightly lower than one and appearing pure by SDS-PAGE were pooled, concentrated, flash-frozen in liquid nitrogen, and stored at −80 °C until further use.

PHM was expressed as described previously (39). The resulting cell paste was sonicated on ice using a Branson sonifier in 30 s pulses for 12 min at 40% output in ~100 mL of 25 mM MOPS pH 7.0, 10% glycerol (Buffer C) containing 100 U of DNaseI (New England Biolabs). Insoluble material was removed by ultracentrifugation at 183,000 x *g* for 60 min., and the supernatant was filtered through a 0.45 μm membrane and loaded onto a Q Sepharose FF column (100 mL) equilibrated in Buffer C. The column was washed with 200 mL of Buffer C, after which bound proteins were eluted in 1 L by running a linear gradient from 0 to 0.5 M NaCl at 1.5 mL/min. PHM eluted in two peaks centered around at ~340 and ~400 mM NaCl that were identified by monitoring the absorbance at 280 nm and by SDS-PAGE and native gel electrophoresis. The contents of fractions corresponding to the first, the second, or both peaks were pooled and concentrated to ~7 mL using a 3K MWCO Amicon centrifugal concentrator (Millipore). The resulting protein was loaded onto a Superdex S75 column equilibrated with Buffer C containing 0.2 M NaCl (Buffer D). Proteins were eluted by running Buffer D over the column at a flow rate of 1 mL/min. PHM eluted in one broad peak with a shoulder. Fractions appearing pure by SDS-PAGE were pooled and concentrated. Properly folded PHM was obtained by thermally denaturing the protein and then letting it refold by slowly cooling the solution to room temperature. For this process, PHM was diluted to 75 μM in 25 mM MOPS, pH 7.0, containing 10% glycerol. The protein was heated to 70 °C over 30 min in a water bath, then the bath was removed from the heating block and the protein allowed to cool until it reached room temperature. The resulting protein was analyzed by native gel electrophoresis, flash-frozen in liquid nitrogen, and stored at −80 °C until further use.

The hydroxylase, ToMOH (42), regulatory, ToMOD (43,44), Rieske, ToMOC (42), and reductase, ToMOF (45), components of ToMO and the ToMOH I100W variant (16,46) were purified as described previously. Specific activities of both PH and ToMO were measured using a coupled assay employing catechol 2,3-dioxygenase and phenol as a substrate (42). Hydroxylase iron content was determined by the ferrozine colorimetric assay (47). Using these procedures, we typically obtained protein activity in the range of 1200-1400 mU/mg for PHH and of 1100-1300 mU/mg for ToMOH, and the iron contents ranged from 3.6-4.1 Fe atoms per dimer for PHH and 3.9-4.1 Fe atoms per dimer for ToMOH. Approximate extinction coefficients used to quantify the PH hydroxylase, regulatory, and reductase proteins were calculated from primary amino acid sequences as 600,000 M^{-1} cm^{-1}, 12,000 M^{-1} cm^{-1}, and 21,000 M^{-1} cm^{-1}, respectively, at 280 nm. Approximate extinction coefficients used to quantify the ToMO hydroxylase and regulatory proteins, calculated from primary amino acid sequences, were 600,000 M^{-1} cm^{-1} and 2,860 M^{-1} cm^{-1}, respectively, at 280 nm. Extinction coefficients used to quantify the ToMO reductase and Rieske protein were previously reported (42).

Single Turnover Assays

To quantify the amount of catechol formed during a single enzyme turnover, we first reduced the appropriate hydroxylase protein in the presence of catechol and the cognate component proteins to generate the O_2-reactive diiron(II) cofactor. We then exposed the reduced solution to O_2 to initiate the oxygenation reaction. After a 20-min incubation, reaction mixtures were assayed for aromatic product content using HPLC.

PHH or ToMOH, prepared in 400 μL of 0.1 M Tris-HCl, pH 7.5, was reduced in an anaerobic chamber by addition of stoichiometric $Na_2S_2O_4$ or on the benchtop by the addition of stoichiometric NADH in the presence of its cognate auxiliary proteins and phenol. The former procedure allowed us to quantify product in the absence of the electron-transfer proteins PHP or ToMOF and ToMOC because $Na_2S_2O_4$ can reduce the diiron centers of PHH and ToMOH directly. For studies probing PH, reaction solutions contained 100 μM PHH, 0 or 600 μM PHM, 10 or 200 μM PHP, 5 mM phenol, and 200 μM NADH or

$Na_2S_2O_4$. For experiments monitoring ToMO, reaction solutions contained 50 μM ToMOH, 0 or 100 μM ToMOD, 100 μM ToMOC, 5 μM ToMOF, 500 μM phenol, and 50 μM NADH or $Na_2S_2O_4$. Accurate $Na_2S_2O_4$ concentrations were determined by anaerobic titration into $K_3[Fe(CN)_6]$ (48).

Reduced protein mixtures were allowed to react with 100 μL of O_2-saturated buffer for a 20-min incubation period at 25 °C and then quenched by addition of 100 μL of 0.4 M TCA to precipitate the protein. The precipitated protein was removed by centrifugation at 17,110 x *g* for 10 min and the supernatant was assayed for catechol content by HPLC. HPLC experiments were performed at a flow rate of 1 mL/min on a Vydac C_{18} reversed-phase protein and peptide column at 25 °C. The separation program utilized a two-solvent system step gradient consisting of 0.1% HCOOH in ddH_2O (solvent A) and 0.1% HCOOH in methanol (solvent B). Following injection of 100 μL of sample onto the column, unbound material was removed by washing with 98% A for 10 min. The aromatic compounds were then eluted using a linear gradient from 2% to 98% B over 10 min. Absorbance of the eluent was monitored continuously at 280 and 274 nm. Under these conditions, phenol and catechol eluted at 18.5 and 10.1 min, respectively. Peaks corresponding to phenol or catechol were integrated and their content was measured by comparison to a standard curve prepared in the same manner as the test solutions. All experiments were run in triplicate using enzymes prepared from different batches of cell paste.

Single turnover studies probing the allosteric effect of *oxidized* electron-transfer protein on the amount of catechol formed by the hydroxylase diiron center were performed in a similar manner, except that diiron centers of PHH or ToMOH was reduced for 20 min with $Na_2S_2O_4$ prior to addition of the cognate electron-transfer protein (PHP for PH and ToMOC for ToMO) and exposure to O_2-saturated buffer.

H_2O_2 Assays

A colorimetric assay was employed to determine the conditions under which PH and ToMO generate H_2O_2 by uncoupled oxidase activity. For studies monitoring PH, reaction solutions contained 1 μM PHH, 0 or 6 μM PHM, 0.1 or 2 μM PHP, and 200 μM NADH in 500 μL of 0.1 M Tris-HCl, pH 7.5. For reactions probing ToMO, reaction solutions contained 1 μM ToMOH, 0 or 2 μM ToMOD, 2 μM ToMOC, 0.1 μM ToMOF, and 200 μM NADH in 500 μL of 0.1 M Tris-HCl, pH 7.5. All reaction mixtures also contained 10 μM of NH_2OH to inhibit the activity of *E. coli* catalase, which is present as an impurity (49) and which affects BMM H_2O_2 assays performed with recombinant proteins by others (22,50). For reactions employing substrate, the concentration of phenol was 5 mM. All reactions were performed at 25.0 ± 0.1 °C or 4.0 ± 0.5 °C. Reactions were initiated by addition of NADH and quenched after a specified reaction time by addition of 100 μL of 0.4 M TCA to precipitate the protein.

H_2O_2 was quantitated colorimetrically with KSCN and $Fe(NH_4)_2(SO_4)_2{\cdot}6H_2O$ (51). However, because unconsumed NADH interferes with the reported procedure, a step was added to inactivate the reducing agent prior to removing the precipitated protein and assaying the supernatants for H_2O_2. Following addition of TCA, reaction mixtures were heated at 90 °C for 15 min then allowed to cool slowly to room temperature over 45 min. Precipitated protein was then removed by centrifugation at 17,110 x *g* for 5 min and 500 μL of supernatant was transferred to a fresh Eppendorf tube. A 200 μL portion of 10 mM $Fe(NH_4)_2(SO_4)_2{\cdot}6H_2O$ in ddH_2O and 100 μL of 2.5 M KSCN in ddH_2O were added to each Eppendorf tube. The reaction mixtures were stirred and allowed to stand for 5 min before their absorption at 480 nm was monitored. Solutions of H_2O_2 in buffer were treated in the same manner as the enzyme reactions to generate a standard curve. For the standards, the concentration of a freshly prepared H_2O_2 stock solution was determined by measuring the

absorbance at 240 nm (ε_{240} = 43.6 M^{-1} cm^{-1}) (52). Data displaying hyperbolic H_2O_2 generation kinetics were fit to the exponential growth model y = A*exp(−*k*t) + B to obtain the first-order rate constant for H_2O_2 production.

H_2O_2 consumption by PH was monitored in the absence of NADH. Reaction mixtures contained 0 or 1 μM PHH, 0 or 6 μM PHM, 2 μM PHP, 10 μM NH_2OH, and 1 mM phenol in 500 μL of 0.1 M Tris-HCl, pH 7.5. Reactions were initiated by addition of 10 or 50 μM H_2O_2 and were quenched after specified reaction times with 100 μL of 0.4 M TCA to precipitate the protein. Precipitated protein was removed by centrifugation at 17110 x *g* for 5 min and 500 μL of supernatant was assayed for H_2O_2 content as described for the H_2O_2 generation assays.

H_2O_2 and NH_2OH Inactivation Assays

Two methods were used to assay for inactivation of PH by H_2O_2. In the first, reaction solutions containing 0.5 μM PHH, 3 μM PHM, and 1 μM PHP in 500 μL of 0.1 M Tris-HCl, pH 7.5 were incubated with 0 or 50 μM H_2O_2 and 1 mM phenol for 20 min. Subsequently, 1 mM NADH was added to initiate the hydrocarbon oxidation reaction. These reactions were quenched after a specified time by addition of 100 μL 0.4 M TCA to precipitate the protein, and the supernatant was assayed for catechol content by HPLC. Plots of catechol formed versus time incubated with H_2O_2 were fit to the linear equation y = *k*x + b to obtain the protein activity.

For the second method, reaction solutions containing 1 μM PHH, 6 μM PHM, and 2 μM PHP in 500 μL of 0.1 M Tris-HCl, pH 7.5 were incubated with 5 mM NADH for a specified time period, after which phenol was added to a final concentration of 5 mM. Reactions were allowed to proceed for 20 min and then were quenched by the addition of 100 μL of 0.4 M TCA to precipitate the protein, and the supernatant was assayed for catechol content by HPLC. Data were plotted as the percentage of the amount of catechol formed in experiments in which NADH and phenol were added simultaneously (*t* = 0 min) versus the time that the reaction mixture was incubated with NADH before addition of phenol.

To determine whether addition of the *E. coli* catalase inhibitor NH_2OH affects activity of PH and ToMO, activity assays were performed in its presence and absence. For PH, reaction solutions contained 2 μM PHH, 12 μM PHM, 4 μM PHP, 1 mM phenol, and 0 or 20 μM NH_2OH in 250 μL of 0.1 M Tris-HCl, pH 7.5. Aliquots of 350 μM NADH were added to initiate hydrocarbon oxidation. Reactions were quenched after 2 or 10 min by addition of 100 μL 0.4 M TCA to precipitate the protein, and the supernatants were assayed for catechol by HPLC. For ToMO, reaction solutions contained 1 μM ToMOH, 4 μM ToMOD, 2 μM ToMOC, 0.1 μM ToMOF, 2 mM phenol, and 0 or 10 μM NH_2OH in 500 μL of 0.1 M Tris-HCl, pH 7.5. Aliquots of 500 μM NADH were added to initiate hydrocarbon oxidation. Reactions were quenched after 1, 5 or 15 min after reaction initiation by addition of 100 μL of 0.4 M TCA to precipitate the protein, and the supernatants were assayed for catechol by HPLC.

NADH Consumption Assays

For studies probing PH, reaction mixtures contained 0 or 1 μM PHH, 0 or 6 μM PHM, 0.1 or 2 μM PHP, and 200 μM NADH in 600 μL of 0.1 M Tris-HCl, pH 7.5. For experiments monitoring ToMO, reaction solutions contained 0 or 1 μM ToMOH, 0 or 2 μM ToMOD, 2 μM ToMOC, 0.1 μM ToMOF, and 200 μM NADH in 500 μL of 0.1 M Tris-HCl, pH 7.5. For reactions containing substrate, the concentration of phenol was 5 mM. All reactions were initiated by addition of PHP for PH and NADH for ToMO. NADH consumption was monitored continuously by absorbance at 340 nm (ε_{340} = 6220 M^{-1} cm^{-1}). Reactions were

thermostatted at 25.0 ± 0.1 °C using a circulating water bath. Data were analyzed by fitting the initial time points to the linear function y = *k*x + b.

RESULTS

Toluene/*o*-xylene monooxygenase (ToMO) and phenol hydroxylase (PH) from *Pseudomonas* sp. OX1 are BMMs responsible for catalyzing the first two steps in the metabolism of benzene, phenol, and other aromatics that can serve as the sole source of carbon and energy for the organism. These enzyme systems must orchestrate the delivery of four substrates, an aromatic hydrocarbon, dioxygen, protons, and electrons, to their carboxylate-bridged diiron centers in the hydroxylase components, where conversion to an aryl alcohol and water occurs. This process requires two or three additional components in addition to the hydroxylase. In the present study we conducted a series of experiments aimed at investigating the possibility that these components might affect more than one of the steps in the catalytic cycle, thereby playing multiple roles in these systems.

We maintained the ratios of protein components employed in all assays reported here to be those reported to yield the best conversion rates of phenol to catechol in steady state experiments. For ToMO, maximal product formation rates occur with 2 equiv of regulatory protein ToMOD, 2 equiv of Rieske protein ToMOC, and 0.1 equiv of reductase ToMOF per hydroxylase dimer (42). For most studies, 2 equiv of ToMOD per ToMOH were used; however, because ToMOD does not inhibit steady state activity as noted for other BMM regulatory proteins (42), experiments employing higher ratios of ToMOD were also conducted and are directly comparable to those employing 2 equiv of ToMOD. For PH expressed from the pGEM3Z/PHΔMΔP vector and used throughout these studies, maximal product formation occurred with ~ 6 equiv of PHM (Figure S1a) and 2 equiv of PHP (data not shown) per hydroxylase dimer.

Single Turnover Assays

In these experiments we wished to determine whether the enzyme systems operate by a half- or full-sites mechanism. Both ToMOH and PHH are dimers and we were interested to learn whether the two protomers would act individually (half-sites) or independently of one another (full-sites). We also were interested to define the minimal number of components necessary to achieve this reaction during a single turnover. For example, although the reductases are not required, does their presence affect the outcome of the reactions?

We first quantified the amount of catechol product formed by various component mixtures during a single enzyme single turnover using phenol as the substrate (Table 1). A negligible amount of catechol was generated by the hydroxylase proteins PHH or ToMOH when they were reduced with $Na_2S_2O_4$ in the absence of their respective auxiliary proteins (<10% per diiron sites). Addition of the regulatory protein, PHM or ToMOD, to the cognate hydroxylase prior to reduction of the diiron centers did not significantly enhance product yield (Table 1). For PH, addition of the reductase (PHP) to PHH before reduction with $Na_2S_2O_4$ improved the product yield, although the amount of catechol formed, 8 ± 3 % per diiron sites, is too low to be physiologically relevant. In similar experiments, the ToMO Rieske protein, ToMOC, did not substantially affect the amount of catechol formed by ToMOH.

Only the fully reconstituted systems containing the hydroxylase, regulatory protein, reductase, and Rieske protein for ToMO generated a significant amount of catechol. Both PH and ToMO formed only ~50% of catechol with respect to protein active site clusters even though the phenolic substrate was present in great excess, indicating a half-sites

reactivity (Table 1). Formation of an active protein ternary complex prior to reduction of the hydroxylase diiron centers presumably mediates efficient product formation.

The results were independent of the electron-transfer mechanism employed, because addition of either NADH, which reduces the hydroxylase active sites via the electron-transfer proteins, or $Na_2S_2O_4$, which directly reduces the diiron centers, generated the same amount of catechol (Table 1). Therefore, low product yields achieved using $Na_2S_2O_4$ with incomplete systems (vide supra) are a consequence of the protein complexation state rather than the use of a non-physiological reduction procedure.

Because complete (~50%) product yields are achieved when the diiron centers are reduced directly with $Na_2S_2O_2$ in the presence of the electron-transfer proteins, but not in their absence, we surmise that these components influence the active hydroxylase conformation through allosteric effects. To investigate this phenomenon more fully, single turnover experiments were conducted in which the diiron centers of a hydroxylase/regulatory protein mixture were reduced with stoichiometric $Na_2S_2O_4$ prior to addition of oxidized electron-transfer protein (PHP for PH or ToMOC for ToMO) to the reaction mixture and subsequent exposure to O_2. Inclusion of the appropriate electron-transfer protein in these experiments significantly enhanced product yield. For PH, the yield of catechol increased from undetectable levels in the absence of PHP to 24 ± 6 % of the diiron centers in its presence. For ToMO, a 3-fold increase in product yield was promoted by inclusion of ToMOC. Although these results clearly demonstrate that the oxidized electron-transfer protein plays a role in the phenol oxidation process happening at the hydroxylase diiron centers, it is important to note that maximal (~50%) product accumulation did not occur either enzyme system.

Steady State NADH Consumption by PH and ToMO

We also examined the effects of the auxiliary proteins on steady state catalysis. Table 2 shows the rates of NADH consumption during steady state turnover in the PH and ToMO systems at 25 °C and 4 °C (data not shown) under a variety of conditions. PHH and ToMOH do not consume NADH in the absence of their cognate electron-transfer proteins. Consumption of NADH by the electron-transfer proteins PHP or ToMOC and ToMOF occurs at very modest rates, presumably by uncoupled oxidase activity and generation of H_2O_2 (vide infra). NADH consumption by the PH and ToMO electron-transfer protein/hydroxylase complexes is more rapid than for the electron-transfer protein(s) alone, probably because transfer of electrons from the electron-transfer protein to the hydroxylase leads to more rapid regeneration of the oxidized electron-transfer protein, which is then ready to acquire more electrons from NADH. Alternatively, the electron-transfer proteins could assume a conformation that accepts electrons more readily when complexed with their cognate hydroxylase.

Of consequence is the finding that the rates of NADH consumption by the electron-transfer protein/hydroxylase mixture are accelerated by two- to three-fold with the inclusion of the cognate regulatory protein, a phenomenon also observed in sMMO (20). This result suggests that the regulatory proteins play a role in the electron-transfer process, at least when hydrocarbon substrate is not present. As expected, the rates of NADH consumption are significantly enhanced by the presence of the substrate phenol because aromatic hydrocarbon oxidation leads to rapid regeneration of the oxidized protein components.

Steady State H_2O_2 Production PH and ToMO

NADH consumption experiments clearly demonstrated that PH and ToMO consume electrons in the absence of hydrocarbon substrate (vide supra), and we wished to determine

the fate of these reducing equivalents. If these electrons are used to catalyze the two-electron reduction of O_2 to H_2O_2 or the four-electron reduction of O_2 to H_2O, an important insight into the catalytic mechanisms of these protein systems is provided. We therefore performed steady state experiments to quantify the amount of H_2O_2 produced by PH and ToMO under a variety of conditions. Although we cannot compare quantitatively the results of these experiments to the NADH consumption studies because of differences in the experimental protocols, the results afford a qualitative assessment of the reaction chemistry accessible to the systems.

It is already known that some BMMs generate H_2O_2 catalytically in the absence of hydrocarbon substrate (15,20,50); however, the mechanism of H_2O_2 formation by these systems is largely unexplored. Production of H_2O_2 might arise from two sources: (i) oxidase activity of the electron trasnfer protein(s), or (ii) protonation and liberation from peroxodiiron(III) intermediates generated at the hydroxylase diiron active sites during the activation of O_2 (15,17). To distinguish between mechanisms (i) and (ii) we measured the ability of various protein mixtures to produce H_2O_2. The *E. coli* catalase inhibitor NH_2OH was included in all assays to prevent complications of H_2O_2 generation or consumption by trace *E. coli* catalase impurities (50). Importantly, NH_2OH does not interfere with the enzymatic activity of PH or ToMO (data not shown).

Initial attempts to quantify H_2O_2 produced by PH and ToMO utilized a colorimetric method employing KSCN and an Fe(II) source (51). However, this procedure had to be modified because unconsumed NADH present in the reaction mixtures interfered with formation of the colored isothiocyanatoiron(III) complex in a complex manner (Figure S2a). A method was therefore developed to inactivate the reducing agent prior to H_2O_2 quantitation. Although H_2O_2 is reasonably stable to heat for short time periods (~ 1 hr) under acidic conditions, NADH can be inactivated when exposed to low pH and elevated temperatures (53). Accordingly, the quenched reaction mixtures were acidified and heated as described in Materials and Methods before the precipitated protein was removed by centrifugation and the supernatant was assayed for H_2O_2 content. Using this method, a hydrogen peroxide standard curve was found to be independent of NADH concentration (Figure S2b).

With this revised method, we verified that H_2O_2 is generated by the complete PH and ToMO systems in the absence of phenol (Figure 1, diamonds, solid lines). In the presence of phenol, H_2O_2 is not generated by either system (Figure 1, circles, dashed lines), probably because electron consumption is fully coupled to hydrocarbon oxidation. The H_2O_2 evolution profiles of PH and ToMO in the absence of phenol displayed hyperbolic behavior with non-zero y-intercepts. The small amount of apparent H_2O_2 present in the assay mixtures at time zero probably results from protein-bound iron(III) that dissociates upon acid precipitation and then binds to thiocyanate in the reaction mixture to form isothiocyanatoiron(III) and produce the red color detected. Accordingly, the values on the y-intercept approximate the iron content of the proteins being assayed. Fits of the H_2O_2 profiles to single exponential processes returned first-order rate constants of 1.8 min^{-1} for PH and 6.8 min^{-1} for ToMO.

It is important to note for these studies that PH does not consume H_2O_2 in the absence of phenol. Assays employing a 10- or 50-fold excess of H_2O_2 indicated no consumption of H_2O_2 by the enzyme system over 8 min in the absence or presence of PHM and the presence of NH_2OH (Figure S3). Given these findings, reports that both ToMOH (15) and toluene 2-monooxygenase (T2MO) from *Burkholderia cepacia* G4 (54) can consume H_2O_2 by means of catalase activity are likely to reflect small amounts of catalase protein contaminants rather than hydroxylase activity as a catalase (22, 50).

The observed hyperbolic behavior of the PH and ToMO H_2O_2 evolution profiles is most likely due to enzyme inactivation by the hydrogen peroxide that is generated, as previously reported for phenol hydroxylase from *Pseudomonas* sp. CF600 (55). To examine whether PH is indeed inactivated over the course of the reaction, we treated the enzyme system with NADH for up to 8 min before adding phenol, incubating for 20 min, and assaying the reaction mixture for catechol content. Catechol yield decreased as a function of NADH-enzyme incubation time, indicating that time-dependent protein inactivation does indeed occur under the conditions employed in the steady state H_2O_2 assays (Figure 2). To determine whether the observed enzyme inactivation could be mediated by formation of H_2O_2, the enzyme system was incubated with a 100-fold excess of H_2O_2 for 20 min prior to assaying for catechol content. HPLC quantification revealed that the H_2O_2-exposed system generated only 63% of the catechol observed for the untreated enzyme. Together, these results indicate that the hyperbolic nature of the H_2O_2 generation curve results from enzyme inactivation by H_2O_2. We note that the enzyme inactivation process observed in these studies seems to occur more slowly than the H_2O_2 generation curve plateaus, but argue that the results of the two experiments can only be compared qualitatively because of inherent differences in experimental conditions, most notably the type of product monitored. The mechanism of enzyme inactivation probably stems from H_2O_2-mediated free radical damage to the PH proteins. Similar behavior is expected for ToMO (15).

To delineate the mechanism of H_2O_2 production by PH, we examined the abilities of the reductase and hydroxylase to independently generate it. PHP produces H_2O_2 in the presence of O_2 and NADH (Figure 3a). The reaction is also characterized by hyperbolic H_2O_2 evolution, and a fit of the data to an exponential growth model revealed a first-order rate constant k of 0.82 min^{-1}. Under similar conditions, PHP does not consume H_2O_2 in the absence of NADH (Figure S4). The measured rate of H_2O_2 formation by two equiv of PHP is insufficient to account for the H_2O_2 formed by the complete enzyme system, however. It is therefore likely that H_2O_2 arises instead from PHH or from PHH *and* PHP. To distinguish between these two possibilities, H_2O_2 assays were performed with PHH, 6 equiv of PHM, and 0.1 equiv of PHP. At this sub-stoichiometric ratio of PHP to PHH, electron consumption and product formation are fully coupled (39) and oxidase activity of the reductase protein should be negligible. These conditions led to H_2O_2 release from the hydroxylase in a hyperbolic fashion with a first-order rate constant k of 0.77 min^{-1} (Figure 3b). However, the rate of H_2O_2 production under these conditions is also insufficient to account for the H_2O_2 generation profile observed in the presence of the complete, stoichiometric enzyme system. We therefore conclude that H_2O_2 arises from *both* PHP oxidase activity and from generation at the hydroxylase diiron centers with the fully reconstituted system.

In contrast to PH, H_2O_2 evolution from ToMO occurs only from the hydroxylase diiron center. Because the fully coupled experiments employed sub-stoichiometric amounts of reductase (ToMOF) and because ET from ToMOC to ToMOH is rapid (56), it is unlikely that substantial amounts of H_2O_2 results from oxidase activity of these proteins. To verify this hypothesis, we measured the H_2O_2 generation by the complete system in which ToMOH was replaced by its I100W variant, which has a tryptophan residue installed near the enzyme active site and undergoes a different O_2 activation pathway than wild-type hydroxylase. Although both ToMOH and its I100W variant form a peroxodiiron(III/III) intermediate upon reaction of reduced protein with O_2, that generated by ToMOH I100W decays via a one electron-transfer pathway to form a W· and a mixed-valent diiron(III/IV) species (46) rather than directly proceeding to the the diiron(III) resting enzyme state as observed for wild-type species (15). The W· is then quenched via recombination with a hydroxyl radical originating from the diiron center. As a result, ToMOH I100W is not catalytic and demonstrates a negligible specific activity.

H_2O_2 assays employing ToMOH I100W displayed a significantly diminished rate of H_2O_2 formation compared to those using wild-type ToMOH, with $k = 0.84$ min^{-1}, and a marked decrease in the total amount of H_2O_2 generated relative to that of the wild-type protein (Figure 4). These observations suggest that the hydroxylase is the component of the system responsible for generating H_2O_2. The decreased rate of H_2O_2 produced by ToMOH I100W is attributed to the competing process of intermediate decay, which will not produce H_2O_2. Similarly, the diminished amount of H_2O_2 produced by ToMOH I100W is attributed to its inability to engage in catalytic reaction behavior.

DISCUSSION

The remarkable ability of BMM systems to perform challenging hydrocarbon oxidation reactions in a regioselective manner depends on the coordinated efforts of three or more protein components. Regulation of the dynamic interplay between these proteins is crucial to maintaining effective and sustainable enzyme systems. However, these protein interactions are complicated and the functions of the individual protein components are still not fully understood.

Evidence for Half-Sites Reactivity in PH and ToMO

The observations that the complete PH or ToMO systems generate ~50% of product per active sites in single turnover assays (Table 1) and that fewer than 50% of the diiron sites proceed though the common peroxodiiron(III) intermediate thought to be responsible for arene oxidation during O_2 activation (15,17) indicate that these proteins react by a half-sites reactivity mechanism. In this model, negative cooperativity between the two active site protomers assures a mechanism in which only one subunit of the dimer activate O_2 at a time. Such allosteric communication ensures that the other active site is simultaneously engaged in the reductive phase of the catalytic cycle. In support of this mechanism, the crystal structure of the PHH/PHM complex revealed a regulatory protein bound only at one side of the hydroxylase dimer (31), suggesting that one active site in the dimer proceeds through the catalytic cycle at a time2. In contrast, MMOH does not proceed by a half-sites type of mechanism, because 90-100% of product forms per diiron sites in single turnover assays (38).

Electron-Transfer Proteins Regulate Hydroxylase Chemistry

Single turnover experiments reveal that BMM electron-transfer proteins affect the O_2 activation/substrate oxidation steps of catalysis as well as reducing the hydroxylase diiron sites, because the product yield is greatly enhanced by the presence of these proteins even when physiological electron transfer is not operative (Table 1). This conclusion is highlighted by results from single turnover assays in which addition of oxidized electron-transfer protein to a pre-reduced hydroxylase/regulatory protein mixture generated more product than that obtained from reduced hydroxylase/regulatory protein (Table 1). Although maximal (~50%, vide infra) catechol accumulation does not occur under these conditions, the amount of product formed is significantly greater than that generated in the absence of the appropriate ET protein. Because ET from the reductase to the hydroxylase should not occur under these conditions, the enhancement in product yield must arise solely from allosteric effects. The mechanism(s) by which the electron-transfer protein regulates phenol oxidation is unknown; however, studies from sMMO suggest that the binding of MMOR

[2]X-ray crystal structures of oxidized and reduced hydroxylase-regulatory protein complexes from *Pseudomonas mendocina* KR1 toluene 4-monooxygenase reveal one equiv of regulatory protein bound to each protomer of the hydroxylase, however (Bailey, L. J., McCoy, J. G., Phillips Jr., G. N., and Fox, B. G. (2008) *Proc. Natl. Acad. Sci. USA 105*, 19194-19198). The reason for this difference is unknown.

induces a long-lived conformational change in MMOH (27,32,33) and that MMOR modulates product regiospecificity, presumably by altering hydroxylase-substrate interactions (27). The PH and ToMO ET proteins might therefore affect hydroxylase activity by opening a conformationally responsive substrate gate. In the presence of the appropriate electron-transfer protein, the hydroxylase would assume a conformational setting in which hydrocarbon substrates can more readily access the active site. Recent structural studies of the T4mo hydroxylase/regulatory protein (30) indicate that hydrocarbon substrate must enter the active site prior to binding of the regulatory protein, before or during reduction of the hydroxylase, adding further support for this argument.

The regulatory roles of the ET proteins have a more marked effect in PH and ToMO than in sMMO, because single turnover product yields are more significantly affected by the presence of the regulatory protein than in sMMO. PHH or ToMOH alone cannot catalytically generate a significant amount of product; however, reduced sMMO hydroxylase, MMOH, produces ~40% propylene oxide per diiron sites in single turnover reactions using propylene as substrate and ~80% in the presence of the regulatory protein, MMOB (38). MMOR also slightly enhances the product yield in these experiments. Addition of 0.5 equiv of MMOR to a mixture of MMOH and MMOB prior to protein reduction by $Na_2S_2O_4$ only increases the product yield from ~80% to ~88% (38), a smaller and less significant effect than in PH or ToMO. The reasons for the differences between PH/ToMOH and sMMO are unknown, but because it is likely that the mechanisms of hydrocarbon substrate ingress differ between these systems (57), conformational changes in the hydroxylase induced by binding of the electron-transfer protein could regulate hydrocarbon substrate entry.

Regulatory Proteins Regulate ET

The present experiments revealed that NADH consumption by PH and ToMO is retarded in the absence of the regulatory protein when hydrocarbon substrate is not present (Table 2). Similar studies have been reported for sMMO (20). These results implicate the regulatory protein in the ET process, although the molecular details of this process are not understood. X-ray crystal structures of hydroxylase/regulatory protein complexes from *Pseudomonas* sp. OX1 PH (31) and *Pseudomonas mendocina* KR1 T4mo (30) show that the regulatory protein binds to the hydroxylase at the proposed docking site of the cognate electron-transfer protein. It is likely that the regulatory protein promotes a long-lived conformational change in the hydroxylase that persists after its dissociation and facilitates ET protein binding and/or electron transfer to the hydroxylase diiron centers (30). A similar role of the sMMO regulatory protein has been proposed (32).

H_2O_2 Generation by BMMs

In the presence of hydrocarbon substrate, H_2O_2 is not produced by PH or ToMO (Scheme 2) because all reducing equivalents are used productively to form hydroxylated product and H_2O (Scheme 2a). In the absence of hydrocarbon substrate, however, PH and ToMO generate H_2O_2. Under the conditions employed in the experiments, production of H_2O_2 results from the hydroxylase (Scheme 2b), and, in the case of PH, from oxidase activity of the reductase protein (Scheme 2c).

Previous studies probing the reactions of chemically reduced PHH (17) or ToMOH (15) with O_2 in the presence of the appropriate regulatory protein revealed that long-lived peroxodiiron(III) intermediate species with unique spectroscopic and optical characteristics accumulate and decay to a diiron(III) product without forming any high-valent iron species (Scheme 3). This species is thought to be responsible for rapid oxidation of hydrocarbon substrate (15). The studies presented in this work indicate that decay of the peroxodiiron(III)

transients will occur by protonation and liberation of the bound peroxide unit as H_2O_2 in the absence of hydrocarbon substrate. Consistent with this proposal is the observation that sMMO does not produce H_2O_2 under steady-state conditions (20). In this system, the second peroxodiiron(III) intermediate that accumulates, H_{peroxo}, rapidly converts to the di(μ-oxo)diiron(IV) species Q, which can decay by acquiring two electrons and two protons to release H_2O and form the diiron(III) resting state (20,58).

In the context of the cell, the choice of whether the reducing equivalents are used to generate hydroxylated product and H_2O or H_2O_2 is under kinetic control for PH and ToMO: much slower kinetics of H_2O_2 formation (Figure 1) relative to catechol formation (39,42) (Figure S1) ensures that electrons are not used unproductively to generate H_2O_2 when the hydrocarbon substrate is present (Scheme 3). This kinetic effect might reflect a thermodynamic preference of the system for an un- or mono-protonated peroxoiiron(III) species rather than its diprotonated form, enforced by the electrostatic environment of the enzyme active sites. In this manner, the enzymes have evolved to control the product outcome such that only productive hydroxylated product is formed in the presence of hydrocarbon substrate.

CONCLUDING REMARKS

In conclusion, the present experiments reveal that the auxiliary proteins of PH and ToMO affect catalysis in a well-controlled manner. The regulatory proteins PHM and ToMOD accelerate ET, and the ET proteins regulate substrate oxidation. Unraveling the details of the molecular mechanisms underlying these dynamic protein interactions is of crucial importance for understanding these remarkable systems in future studies.

Supplementary Material

Refer to Web version on PubMed Central for supplementary material.

Acknowledgments

We thank Dr. Rachel K. Behan for helpful discussions.

REFERENCES

1. Murray LJ, Lippard SJ. Substrate Trafficking and Dioxygen Activation in Bacterial Multicomponent Monooxygenases. Acc. Chem. Res. 2007; 40:466–474. [PubMed: 17518435]
2. Sazinsky MH, Lippard SJ. Correlating Structure with Function in Bacterial Multicomponent Monooxygenases and Related Diiron Proteins. Acc. Chem. Res. 2006; 39:558–566. [PubMed: 16906752]
3. Leahy JG, Batchelor PJ, Morcomb SM. Evolution of the Soluble Diiron Monooxygenases. FEMS Microbiol. Rev. 2003; 27:449–479. [PubMed: 14550940]
4. Notomista E, Lahm A, Di Donato A, Tramontano A. Evolution of Bacterial and Archaeal Multicomponent Monooxygenases. J. Mol. Evol. 2003; 56:435–445. [PubMed: 12664163]
5. Wallar BJ, Lipscomb JD. Dioxygen Activation by Enzymes Containing Binuclear Non-Heme Iron Clusters. Chem. Rev. 1996; 96:2625–2657. [PubMed: 11848839]
6. Brazeau BJ, Lipscomb JD. Kinetics and Activation Thermodynamics of Methane Monooxygenase Compound Q Formation and Reaction with Substrates. Biochemistry. 2000; 39:13503–13515. [PubMed: 11063587]
7. Tinberg CE, Lippard SJ. Revisiting the Mechanism of Dioxygen Activation in Soluble Methane Monooxygenase from *M. capsulatus* (Bath): Evidence for a Multi-Step, Proton-Dependent Reaction Pathway. Biochemistry. 2009; 48:12145–12158. [PubMed: 19921958]

8. Liu KE, Valentine AM, Wang D, Huynh BH, Edmondson DE, Salifoglou A, Lippard SJ. Kinetic and Spectroscopic Characterization of Intermediates and Component Interactions in Reactions of Methane Monooxygenase from *Methylococcus capsulatus* (Bath). J. Am. Chem. Soc. 1995; 117:10174–10185.
9. Liu KE, Wang D, Huynh BH, Edmondson DE, Salifoglou A, Lippard SJ. Spectroscopic Detection of Intermediates in the Reaction of Dioxygen with Reduced Methane Monooxygenase Hydroxylase from *Methylococcus capsulatus* (Bath). J. Am. Chem. Soc. 1994; 116:7465–7466.
10. Valentine AM, Stahl SS, Lippard SJ. Mechanistic Studies of the Reaction of Reduced Methane Monooxygenase Hydroxylase with Dioxygen and Substrates. J. Am. Chem. Soc. 1999; 121:3876–3887.
11. Lee S-K, Lipscomb JD. Oxygen Activation Catalyzed by Methane Monooxygenase Hydroxylase Component: Proton Delivery during the O—O Bond Cleavage Steps. Biochemistry. 1999; 38:4423–4432. [PubMed: 10194363]
12. Lee S-K, Fox BG, Froland WA, Lipscomb JD, Münck E. A Transient Intermediate of the Methane Monooxygenase Catalytic Cycle Containing an $Fe^{IV}Fe^{IV}$ Cluster. J. Am. Chem. Soc. 1993; 115:6450–6451.
13. Lee S-K, Nesheim JC, Lipscomb JD. Transient Intermediates of the Methane Monooxygenase Catalytic Cycle. J. Biol. Chem. 1993; 268:21569–21577. [PubMed: 8408008]
14. Shu L, Nesheim JC, Kauffmann K, Münck E, Lipscomb JD, Que L Jr. An $Fe_2^{IV}O_2$ Diamond Core Structure for the Key Intermediate Q of Methane Monooxygenase. Science. 1997; 275:515–518. [PubMed: 8999792]
15. Murray LJ, Naik SG, Ortillo DO, García-Serres R, Lee JK, Huynh BH, Lippard SJ. Characterization of the Arene-Oxidizing Intermediate in ToMOH as a Diiron(III) Species. J. Am. Chem. Soc. 2007; 129:14500–14510. [PubMed: 17967027]
16. Murray LJ, García-Serres R, Naik S, Huynh BH, Lippard SJ. Dioxygen Activation at Non-Heme Diiron Centers: Characterization of Intermediates in a Mutant Form of Toluene/o-Xylene Monooxygenase Hydroxylase. J. Am. Chem. Soc. 2006; 128:7458–7459. [PubMed: 16756297]
17. Izzo V, Tinberg CE, García-Serres R, Naik S, Huynh BH, Lippard SJ. 2010 Manuscript in Preparation.
18. Merkx M, Kopp DA, Sazinsky MH, Blazyk JL, Müller J, Lippard SJ. Dioxygen Activation and Methane Hydroxylation by Soluble Methane Monooxygenase: A Tale of Two Irons and Three Proteins. Angew. Chem. Int. Ed. 2001; 40:2782–2807.
19. Fox BG, Liu Y, Dege JE, Lipscomb JD. Complex Formation between the Protein Components of Methane Monooxygenase from *Methylosinus trichosporium* OB3b: Identification of Sites of Component Interaction. J. Biol. Chem. 1991; 266:540–550. [PubMed: 1845980]
20. Gassner GT, Lippard SJ. Component Interactions in the Soluble Methane Monooxygenase System from *Methylococcus capsulatus* (Bath). Biochemistry. 1999; 38:12768–12785. [PubMed: 10504247]
21. Green J, Dalton H. Protein B of Soluble Methane Monooxygenase from *Methylococcus capsulatus* (Bath): A Novel Regulatory Protein of Enzyme Activity. J. Biol. Chem. 1985; 260:15795–15801. [PubMed: 3934164]
22. Pikus JD, Studts JM, Achim C, Kauffmann KE, Münck E, Steffan RJ, McClay K, Fox BG. Recombinant Toluene-4-monooxygenase: Catalytic and Mössbauer Studies of the Purified Diiron and Rieske Components of a Four-Protein Complex. Biochemistry. 1996; 35:9106–9119. [PubMed: 8703915]
23. Liu KE, Lippard SJ. Redox Properties of the Hydroxylase Component of Methane Monooxygenase from *Methylococcus capsulatus* (Bath): Effects of Protein B, Reductase, and Substrate. J. Biol. Chem. 1991; 266:12836–12839. [PubMed: 1649166]
24. Paulsen KE, Liu Y, Fox BG, Lipscomb JD, Münck E, Stankovich MT. Oxidation-Reduction Potentials of the Methane Monooxygenase Hydroxylase Component from *Methylosinus trichosporium* OB3b. Biochemistry. 1994; 33:713–722. [PubMed: 8292599]
25. DeWitt JG, Rosenzweig AC, Salifoglou A, Hedman B, Lippard SJ, Hodgson KO. X-ray Absorption Spectroscopic Studies of the Diiron Center in Methane Monooxygenase in the

Presence of Substrate and the Coupling Protein of the Enzyme System. Inorg. Chem. 1995; 34:2505–2515.

26. Fox BG, Hendrich MP, Surerus KK, Andersson KK, Froland WA, Lipscomb JD, Münck E. Mössbauer, EPR, and ENDOR Studies of the Hydroxylase and Reductase Components of Methane Monooxygenase from *Methylosinus trichosporium* OB3b. J. Am. Chem. Soc. 1993; 115:3688–3701.
27. Froland WA, Andersson KK, Lee S-K, Liu Y, Lipscomb JD. Methane Monooxgenase Component B and Reductase Alter the Regioselectivity of the Hydroxylase Component-catalyzed Reactions: A Novel Role for Protein-Protein Interactions in an Oxygenase Mechanism. J. Biol. Chem. 1992; 267:17588–17597. [PubMed: 1325441]
28. Mitić N, Schwartz JK, Brazeau BJ, Lipscomb JD, Solomon EI. CD and MCD Studies of the Effects of Component B Variant Binding on the Biferrous Active Site of Methane Monooxygenase. Biochemistry. 2008; 47:8386–8397. [PubMed: 18627173]
29. Pulver SC, Froland WA, Lipscomb JD, Solomon EI. Ligand Field Circular Dichroism and Magnetic Circular Dichroism Studies of Component B and Substrate Binding to the Hydroxylase Component of Methane Monooxygenase. J. Am. Chem. Soc. 1997; 119:387–395.
30. Bailey LJ, McCoy JG, Phillips GN Jr. Fox BG. Structural Consequences of Effector Protein Complex Formation in a Diiron Hydroxylase. Proc. Natl. Acad. Sci. USA. 2008; 105:19194–19198. [PubMed: 19033467]
31. Sazinsky MH, Dunten PW, McCormick MS, Di Donato A, Lippard SJ. X-ray Structure of a Hydroxylase-Regulatory Protein Complex from a Hydrocarbon-Oxidizing Multicomponent Monooxygenase, *Pseudomonas* sp. OX1 Phenol Hydroxylase. Biochemistry. 2006; 45:15392–15404. [PubMed: 17176061]
32. Blazyk JL, Gassner GT, Lippard SJ. Intermolecular Electron-Transfer Reactions in Soluble Methane Monooxygenase: A Role for Hysteresis in Protein Function. J. Am. Chem. Soc. 2005; 127:17364–17376. [PubMed: 16332086]
33. Gallagher SC, Callaghan AJ, Zhao J, Dalton H, Trewhella J. Global Conformational Changes Control the Reactivity of Methane Monooxygenase. Biochemistry. 1999; 38:6752–6760. [PubMed: 10346895]
34. Wallar BJ, Lipscomb JD. Methane Monooxygenase Component B Mutants Alter the Kinetic Steps Throughout the Catalytic Cycle. Biochemistry. 2001; 40:2220–2233. [PubMed: 11329291]
35. Mitchell KH, Studts JM, Fox BG. Combined Participation of Hydroxylase Active Site Residues and Effector Protein Binding in a *Para* to *Ortho* Modulation of Toluene 4-Monooxygenase Regiospecificity. Biochemistry. 2002; 41:3176–3188. [PubMed: 11863457]
36. Zheng H, Lipscomb JD. Regulation of Methane Monooxygenase Catalysis Based on Size Exclusion and Quantum Tunneling. Biochemistry. 2005; 45:1685–1692. [PubMed: 16460015]
37. Liu Y, Nesheim JC, Lee S-K, Lipscomb JD. Gating Effects of Component B on Oxygen Activation by the Methane Monooxygenase Hydroxylase Component. J. Biol. Chem. 1995; 270:24662–24665. [PubMed: 7559577]
38. Liu Y, Nesheim JC, Paulsen KE, Stankovich MT, Lipscomb JD. Roles of the Methane Monooxygenase Reductase Component in the Regulation of Catalysis. Biochemistry. 1997; 36:5223–5233. [PubMed: 9136884]
39. Cafaro V, Izzo V, Scognamiglio R, Notomista E, Capasso P, Casbarra A, Pucci P, Di Donato A. Phenol Hydroxylase and Toluene/*o*-Xylene Monooxygenase from *Pseudomonas stutzeri* OX1: Interplay between Two Enzymes. Appl. Environ. Microbiol. 2004; 70:2211–2219. [PubMed: 15066815]
40. Powlowski J, Shingler V. Genetics and Biochemistry of Phenol Degradation by *Pseudomonas* sp. CF600. Biodegradation. 1994; 5:219–236. [PubMed: 7765834]
41. Arenghi FLG, Berlanda D, Galli E, Sello G, Barbieri P. Organization and Regulation of *meta* Cleavage Pathway Genes for Toluene and *o*-Xylene Derivative Degradation in *Pseudomonas stutzeri* OX1. Appl. Environ. Microbiol. 2001; 67:3304–3308. [PubMed: 11425758]
42. Cafaro V, Scognamiglio R, Viggiani A, Izzo V, Passaro I, Notomista E, Dal Piaz F, Amoresano A, Casbarra A, Pucci P, Di Donato A. Expression and Purification of the Recombinant Subunits of

Toluene/*o*-Xylene Monooxygeanse and Reconsitution of the Active Complex. Eur. J. Biochem. 2002; 269:5689–5699. [PubMed: 12423369]

43. Bertoni G, Martino M, Galli E, Barbieri P. Analysis of the Gene Cluster Encoding Toluene/*o*-Xylene Monooxygenase from *Pseudomonas stutzeri* OX1. App. Environ. Microbiol. 1998; 64:3626–3632.
44. Scognamiglio R, Notomista E, Barbieri P, Pucci P, Dal Piaz F, Tramontano A, Di Donato A. Conformational Analysis of Putative Regulatory Subunit D of the Toluene/*o*-Xylene-Monooxygenase Complex from *Pseudomonas stutzeri* OX1. Protein Sci. 2001; 10:482–490. [PubMed: 11344317]
45. Song WJ, Behan RK, Naik SG, Huynh BH, Lippard SJ. Characterization of a Peroxodiiron(III) Intermediate in the T201S Variant of Toluene/*o*-Xylene Monooxygenase Hydroxylase from *Pseudomonas* sp. OX1. J. Am. Chem. Soc. 2009; 131:6074–6075. [PubMed: 19354250]
46. Murray LJ, García-Serres R, McCormick MS, Davydov R, Naik SG, Kim S-H, Hoffman BM, Huynh BH, Lippard SJ. Dioxygen Activation at Non-Heme Diiron Centers: Oxidation of a Proximal Residue in the I100W Variant of Toluene/*o*-Xylene Monooxygenase Hydroxylase. Biochemistry. 2007; 46:14795–14809. [PubMed: 18044971]
47. Gibbs CR. Characterization and Application of FerroZine Iron Reagent as a Ferrous Iron Indicator. Anal. Chem. 1976; 48:1197–1201.
48. Lambeth DO, Palmer G. The Kinetics and Mechanism of Reduction of Electron Transfer Protein and Other Compounds of Biological Interest by Dithionite. J. Biol. Chem. 1973; 248:6095–6103. [PubMed: 4353631]
49. Switala J, Loewen PC. Diversity of Properties Among Catalases. Arch. Biochem. Biophys. 2002; 401:145–154. [PubMed: 12054464]
50. Elsen NL, Bailey LJ, Hauser AD, Fox BG. Role for Threonine 201 in the Catalytic Cycle of the Soluble Diiron Hydroxylase Toluene 4-Monooxygenase. Biochemistry. 2009; 48:3838–3846. [PubMed: 19290655]
51. Hildebrandt AG, Roots I. Reduced Nicotinamide Adenine Dinucleotide Phosphate (NADPH)-Dependent Formation and Breakdown of Hydrogen Peroxide during Mixed Function Oxidation Reaction in Liver Microsomes. Arch. Biochem. Biophys. 1975; 171:385–397. [PubMed: 955]
52. Messner KR, Imlay JA. *In Vitro* Quantitation of Biological Superoxide and Hydrogen Peroxide Generation. Methods Enzymol. 2002; 349:354–361. [PubMed: 11912927]
53. Yang X, Ma K. Determination of Hydrogen Peroxide Generated by Reduced Nicotinamide Adenine Dinucleotide Oxidase. Anal. Biochem. 2005; 344:130–134. [PubMed: 16039979]
54. Newman LM, Wackett LP. Purification and Characterization of Toluene 2-Monooxygenase from *Burkholderia cepacia* G4. Biochemistry. 1995; 34:14066–14076. [PubMed: 7578004]
55. Cadieux E, Vrajmasu V, Achim C, Powlowski J, Münck E. Biochemical, Mössbauer, and EPR Studies of the Diiron Cluster of Phenol Hydroxylase from *Pseudomonas* sp. Strain CF 600. Biochemistry. 2002; 41:10680–10691. [PubMed: 12186554]
56. Song WJ, Lippard SJ. 2010 Unpublished Results.
57. McCormick, MS. Ph.D. Thesis. Massachusetts Institute of Technology; Cambridge, MA: 2008. Structural Investigations of Hydroxylase Proteins and Complexes in Bacterial Multicomponent Monooxygenase Systems.
58. Lund J, Woodland MP, Dalton H. Electron Transfer Reactions in the Soluble Methane Monooxygenase of *Methylococcus capsulatus* (Bath). Eur. J. Biochem. 1985; 147:297–305. [PubMed: 3918864]

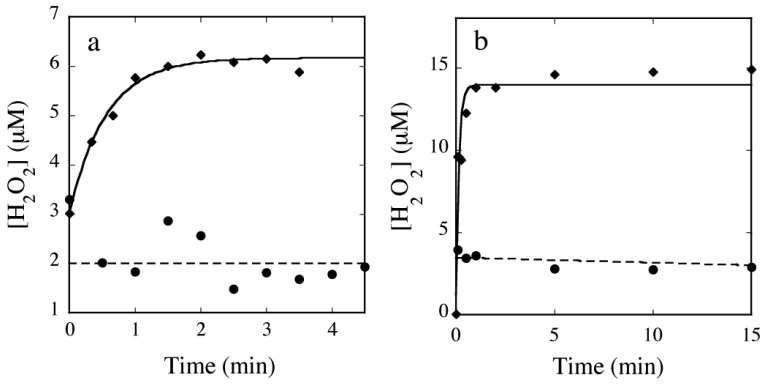

Figure 1.

Representative profiles of H_2O_2 generated by PH (a) and ToMO (b). (a) H_2O_2 generation profile upon addition of 200 μM NADH to a solution of 1 μM PHH, 6 μM PHM, 2 μM PHP, and 10 μM NH_2OH at pH 7.5 and 4 °C in the presence (diamonds, solid lines) or absence (circles, dashed lines) of 5 mM phenol. (b) H_2O_2 generation profile upon addition of 200 μM NADH to a solution of 1 μM ToMOH, 2 μM ToMOD, 2 μM ToMOC, 0.1 μM ToMOF, and 10 μM NH_2OH at pH 7.5 and 4 °C in the presence (diamonds, solid lines) or absence (circles, dashed lines) of 5 mM phenol. Data obtained in the absence of phenol were fit (solid lines) to the single exponential formation process $y = A*\exp(-kt) + B$. Reaction solutions were assayed for H_2O_2 content as noted in the text.

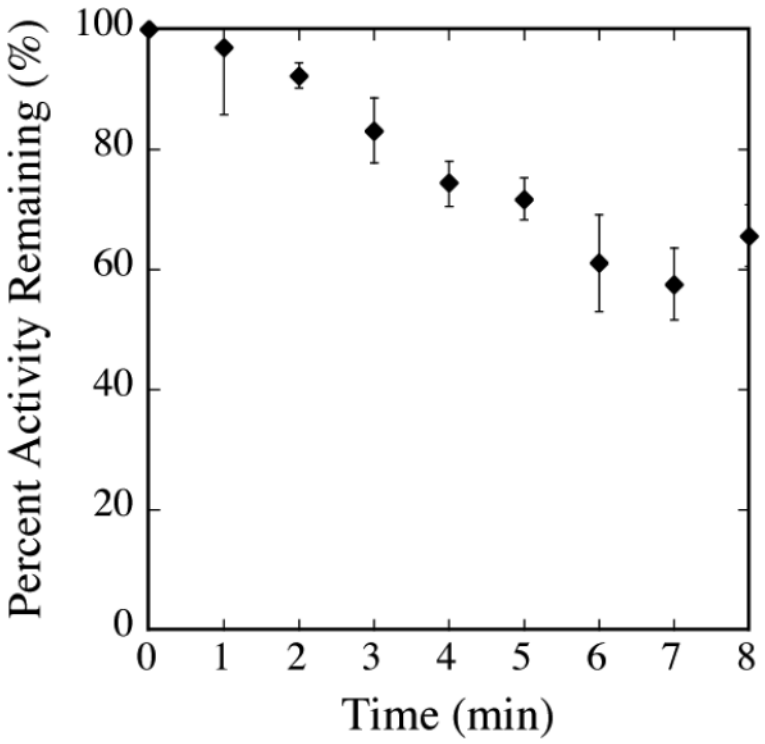

Figure 2.

Percent PH activity remaining as a function of time following incubation with NADH. Reaction solutions containing 1 μM PHH, 6 μM PHM, 2 μM PHP in 500 μL of 0.1 M Tris-HCl, pH 7.5, were incubated with 5 mM NADH for a specified time period between 0 and 8 min, after which 5 mM phenol was added. Reactions were allowed to proceed for 20 min and then were quenched by addition of 100 μL of TCA. Catechol content was monitored by HPLC. Data are plotted as the percentage of the amount of catechol formed in experiments in which NADH and phenol were added simultaneously (t = 0 min) versus the time that the reaction mixture was incubated with NADH before addition of phenol. Data points represent the average of two trials performed with different batches of protein.

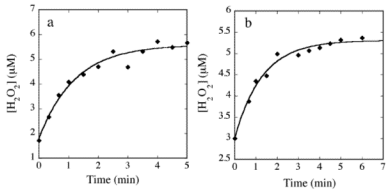

Figure 3.

(a) Representative profile of H_2O_2 generation (diamonds) upon addition of 200 μM NADH to 2 μM PHP at pH 7.5 and 4 °C. Similar reaction profiles were obtained in the presence of NH_2OH. (b) Representative profile of H_2O_2 generation (diamonds) upon addition of 200 μM NADH to a solution of 1 μM PHH, 6 μM PHM, 0.1 μM PHP, and 10 μM NH_2OH at pH 7.5 and 4 °C. Data were fit (solid lines) to the single exponential formation process y = A*exp(−*k*t) + B. Reaction solutions were assayed for H_2O_2 content as noted in the text. See text for comment on the non-zero ordinate intercepts.

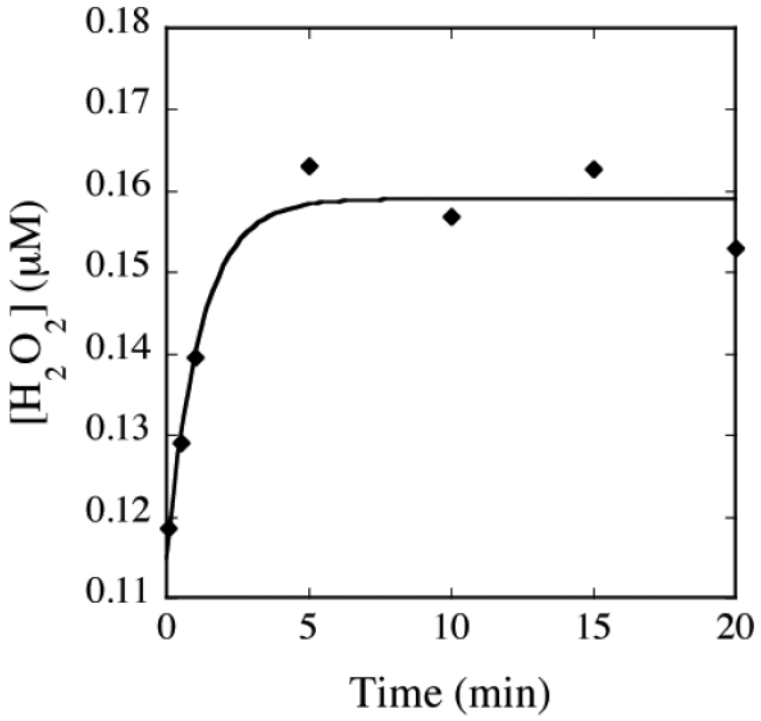

Figure 4.

Representative H_2O_2 generation profile upon addition of 200 μM NADH to a solution of 1 μM ToMOH I100W, 2 μM ToMOD, 2 μM ToMOC, 0.1 μM ToMOF, and 10 μM NH_2OH at pH 7.5 and 25 °C in the absence of phenol. Data were fit (solid lines) to a single exponential formation process, y = A*exp(−*k*t) + B. Reaction solutions were assayed for H_2O_2 content as noted in the text.

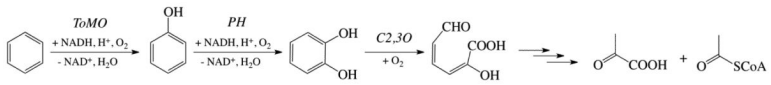

Scheme 1.
Pathway of benzene metabolism by *Pseudomonas* sp. OX1.

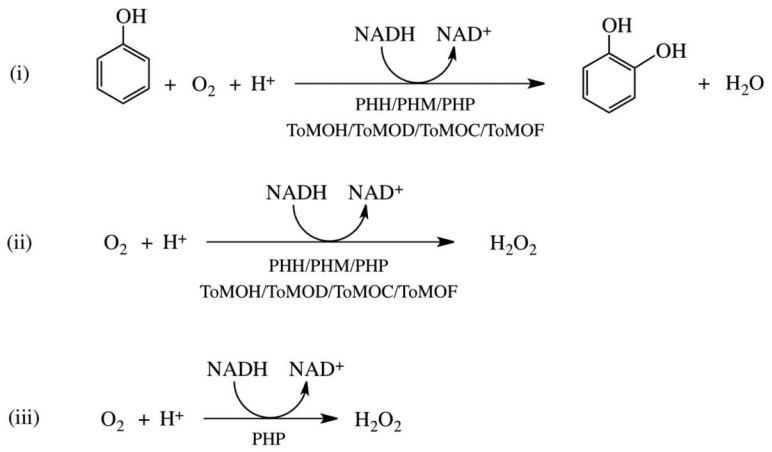

Scheme 2.

Product evolution by PH or ToMO in the presence (i) or absence (ii) of phenol and by PHP in the absence of phenol (iii).

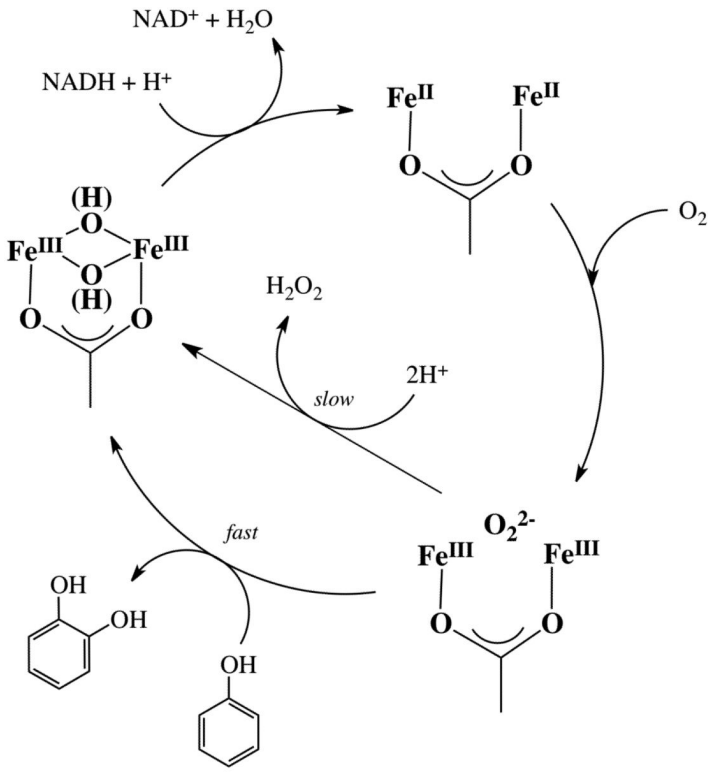

Scheme 3.
Proposed mechanism of O_2 activation by ToMO and PH.

Table 1

Single Turnover Yields[a]

Phenol Hydroxylase (PH)			Toluene/*o*-Xylene Monooxygenase (ToMO)		
Reaction Conditions	**Reducing Agent**	**% Catechol Formed/ Active Sites**	**Reaction Conditions**	**Reducing Agent**	**% Catechol Formed/ Active Sites**
PHH	$Na_2S_2O_4$	nd[b]	ToMOH	$Na_2S_2O_4$	6.9 ± 0.2
PHH:6PHM:2PHP	NADH	54 ± 2	ToMOH:2ToMOD:2ToMOC:0.1ToMOF	NADH	50 ± 7
PHH:6PHM:2PHP	$Na_2S_2O_4$	54 ± 1	ToMOH:2ToMOD:2ToMOC	$Na_2S_2O_4$	46 ± 3
PHH_{red}:6PHM:$2PHP_{ox}$[c]	$Na_2S_2O_4$	24 ± 6	$ToMOH_{red}$:2ToMOD:$2ToMOC_{ox}$[d]	$Na_2S_2O_4$	29 ± 1
PHH:6PHM	$Na_2S_2O_4$	nd[b]	ToMOH:2ToMOD	$Na_2S_2O_4$	10.0 ± 0.9
PHH:2PHP	$Na_2S_2O_4$	8 ± 3	ToMOH:2ToMOC	$Na_2S_2O_4$	11 ± 2

[a] All experiments were performed at 25 °C.

[b] None detected.

[c] PHH:6M was pre-reduced with stoichiometric $Na_2S_2O_4$ prior to adding PHP_{ox}. After subsequent addition of O_2-saturated buffer, the solution was assayed for catechol content.

[d] ToMOH:2D was pre-reduced with stoichiometric $Na_2S_2O_4$ prior to adding $ToMOC_{ox}$. After subsequent addition of O_2-saturated buffer, the solution was assayed for catechol content.

Table 2

NADH Consumption Rates[a]

Phenol Hydroxylase (PH)		Toluene/*o*-Xylene Monooxygenase (ToMO)	
Reaction Conditions	**NADH Consumption Rate (*μ*M/min)**	**Reaction Conditions**	**NADH Consumption Rate (*μ*M/min)**
PHH	nd[b]	ToMOH	nd[b]
PHH:6PHM:2PHP	67.2 ± 0.7	ToMOH:4ToMOD:2ToMOC:0.1ToMOF	14 ± 2
PHH:2PHP	17.6 ± 0.2	ToMOH:4ToMOD	6.4 ± 0.6
PHH:6PHM:2PHP:phenol	180 ± 7	ToMOH:4ToMOD:2ToMOC:0.1ToMOF:phenol	86 ± 5
2PHP	4.0 ± 0.3	0.1ToMOF:2ToMOC	1.9 ± 0.2

[a] All experiments were performed at 25 °C.

[b] No NADH consumption detected.